Available online at www.sciencedirect.com

SCIENCE DIRECT®

Journal of Solid State Chemistry 177 (2004) 4632–4639

JOURNAL OF SOLID STATE CHEMISTRY

www.elsevier.com/locate/jssc

Synthesis of rare-earth selenate and selenite materials under "sol–gel" hydrothermal conditions: crystal structures and characterizations of $La(HSeO_3)(SeO_4)$ and $KNd(SeO_4)_2$

Wei Liu, Hao-Hong Chen, Xin-Xin Yang, Mang-Rong Li, Jing-Tai Zhao*

State Key Laboratory of High Performance Ceramics and Superfine Microstructure, Shanghai Institute of Ceramics, Chinese Academy of Science, Number 1295, Ding Xi Road, Shanghai, 200050, PR China

Received 19 August 2004; received in revised form 27 September 2004; accepted 29 September 2004
Available online 11 November 2004

Abstract

Two rare-earth compounds containing selenium atoms, $La(HSeO_3)(SeO_4)$ with a new open framework structure and $KNd(SeO_4)_2$ with a layered structure, have been synthesized under "sol–gel" hydrothermal conditions for the first time. Single-crystals of $La(HSeO_3)(SeO_4)$ crystallize in the monoclinic system ($P2_1$, $a = 8.5905(17)$ Å, $b = 7.2459(14)$ Å, $c = 9.5691(19)$ Å, $\beta = 104.91(3)^\circ$, $Z = 2$, $R_{All} = 0.032$). The structure contains puckered polyhedral layers made of LaO_x ($x = 9, 10$) and SeO_4 groups, which are connected via SeO_3-uints to the 3D structure. The crytal structure of $KNd(SeO_4)_2$ (monoclinc, $P2_1/c$, $a = 8.7182(17)$ Å, $b = 7.3225(15)$ Å, $c = 11.045(2)$ Å, $\beta = 91.38(3)^\circ$, $Z = 4$, $R_{All} = 0.051$) contains honeycomb-like six-ring NdO_9 polyhedra forming layers which are further decorated with SeO_4 tetrahedra. The K^+ ions occupy the interspaces of these layers and provide the charge balance.

Keywords: Crystal structure; Sol–gel process; Rare earth; Selenates; Selenites

1. Introduction

Rare-earth compounds containing selenium Se(IV) and Se(VI), have been known for well over 100 years [1]. Although the literature and applications of the rare-earth selenates and selenites are not nearly as extensive as those of their phosphor containing counterparts, they have been studied as potential precursors in the synthesis of rare-earth phosphor and as ion exchangers [2]. Of particular interest is the family of selenites due to their stereochemically active lone pair of electrons on the selenium atom. Thus, during the past decades, considerable efforts have been devoted to the investigations on the structure chemistry of selenates and selenites, and yielded a large number of rare-earth selenates and selenites compounds with varied and interesting structures. These have included one-dimensional structures, such as $La_2(SeO_4)_3(H_2O)_{12}$ [3], $RbNd(SeO_4)_2(H_2O)_3$ [4], $CsNd(SeO_4)_2(H_2O)_4$ [5], layered structures, such as $KPr(SeO_4)_2$ [6], $LaH(SeO_3)_2$ [7], $Pr_2(HSeO_3)_2(SeO_3)_2$ [8], and three-dimensional structures such as $La(HSeO_4)_3$ [9], $La(SeO_3)_2$ [10], $NaLa(SeO_3)_2$ [11]. Up to the present day, there have also been three examples of compounds containing both Se(IV) and Se(VI) oxyanions in the crystal structures, $La(HSeO_3)(SeO_4)(H_2O)_2$ [12], $NaSm(SeO_3)(SeO_4)$ [13] and $Er(SeO_3)(SeO_4)_{0.5}(H_2O)$ [14].

Although the hydrothermal method has played an important role in the preparation of the selenates and selenites owing to its advantages with respect to growth and isolation of the single crystals, some disadvantages are obvious. For example, to withstand the pressure involved in hydrothermal synthesis, a special reaction

---

*Corresponding author. Fax: +86 21 5241 3122.
E-mail address: jtzhao@mail.sic.ac.cn (J.-T. Zhao).

0022-4596/$ - see front matter © 2004 Elsevier Inc. All rights reserved.
doi:10.1016/j.jssc.2004.09.038

vessel is usually required to avoid an explosion [15–18]. Therefore, the approaches to reduce the reliance on traditional solvents will be of tremendous importance in solving these problems. In this paper, we report a new synthetic method to prepare new materials in the rare-earth–selenate/selenite system by the sol–gel process under hydrothermal conditions, which interestingly lead to the isolation of the title compounds, La($HSeO_3$)(SeO_4), **1** and KNd(SeO_4)$_2$, **2**, suggesting that this method may be exploited for the preparation of novel compounds in metal-oxo-selenium system and other related systems.

2. Experimental

2.1. Synthesis and characterizations

The reagents used were commercially obtained with analytical purities and used without further purification. The synthesis of the title compounds were prepared as follows: for **1**, 0.326 g of La_2O_3 (acidified with HNO_3), 0.1 g of KOH and 0.65 mL of H_2SeO_4 (40 wt%) were mixed in 5 mL of deioned water in molar ratio 1:2:3, and the solution was stirred for 30 min. After this period, 1.34 mL of $Si(OC_2H_5)_4$ (TEOS) was added gradually to this mixture, and the resulting sol was stirred at a temperature of 353 K till the formation of a wet colorless transparent gel. A similar process was carried out for **2** and a pink transparent wet gel was obtained. These wet gels were sealed in 15 mL Teflon-lined stainless steel autoclaves and heated for 3 days under autogenous pressure at 473 and 483 K for compounds **1** and **2**, respectively. The resulting colorless column-like and pink plate-like crystals, respectively, were isolated from the residue of these gels. The yields were 80% based on La_2O_3 for **1** and 85% based on Nd_2O_3 for **2**.

The products were examined by powder X-ray diffraction (Rigaku D/max 2550 V diffractometer, Cu*K*) in order to confirm their phase identity and purity. The experimental diffraction patterns were in good agreement with the ones calculated from the structures determined by single-crystal X-ray diffraction. The EDS analyses (EPMA_8705QH$_2$ electron microscope equipped with a LINK ISIS) indicated no presence of Si element in both compounds. Elemental analysis by ICP-AES (Varian Vista, radial observation): Found: La, 33.81; Se, 38.59. Calc. for **1**: La, 33.89; Se, 38.53. Found: K, 8.27; Nd, 30.66; Se, 33.72%. Calc. for **2**: K, 8.31; Nd, 30.74; Se, 33.65%.

Infrared spectra were collected on a Digilab-FTS-80 spectrophotometer using KBr pellets of the samples, and showed features consistent with the presence of $(HSeO_3)^{-}$ and $(SeO_4)^{2-}$ anions. Thus, for compound **1**, the peaks at 785, 813, and 435 cm^{-1} were ascribed to the vibrations of SeO_3^{2-}. Peaks observed at the region 915–845 and 416 cm^{-1} are associated with SeO_4^{2-} units. The peak at 1342 cm^{-1} was attributed to the vibrations of the O–H group. For compound **2**, the spectrum exhibits the SeO_4^{2-} vibrations between 846 and 449 cm^{-1}.

2.2. Crystal structure determinations

Crystals from each compound were selected under a polarizing microscope, glued to a thin glass fiber with cyanoacrylate (superglue) adhesive, and inspected for singularity. Two of them were chosen, ($0.20 \times 0.10 \times 0.10$ mm for **1** and $0.30 \times 0.1 \times 0.1$ mm for **2**), and data sets were collected at 295 K on a Nonius Kappa CCD diffractometer equipped with a normal focus, 2.4 kW sealed tube X-ray source (Mo*K*α radiation, $\lambda = 0.71073$ Å) operating at 50 kV and 40 mA. Additional information about the data collection and structure refinement is presented in Table 1. The data were corrected for absorption using the SADABS program [19]. The structures were solved by direct methods and refined against $|F^2|$ with the aid of the SHELXTL-97 package [20]. For **1**, the lanthanum and selenium atoms were located form the structure solution, whereas the oxygen atoms and hydrogen atom were found in the difference Fourier maps. For **2**, all the non-hydrogen atoms were located by the direct methods and subsequently refined anisotropically. The atomic positional and displacement parameters are given in

Table 1
Crystal structure refinement data for La($HSeO_3$)(SeO_4) and KNd(SeO_4)$_2$

Structure param	**1**	**2**
Empirical formula	H2 La2 O14 Se4	K Nd O8 Se2
Formula weight	819.68	469.26
Wavelength (Å)	0.71073	0.71073
Crystal system	Monoclinic	Monoclinic
Space group	$P2_1$	$P2_1/c$
a (Å)	8.5905(17)	8.7182(17)
b (Å)	7.2459(14)	7.3225(15)
c (Å)	9.5691(19)	11.045(2)
β (°)	104.91(3)	91.38(3)
V	575.6(2) Å^3	704.9(2) Å^3
Z	2	4
$D_{(calc)}$ (Mg/m^3)	4.729	4.422
μ(Mo$K\alpha$) (mm^{-1})	20.048	18.289
$F(000)$	728	844
θ range (°)	2.20–27.05	2.34–27.08
Total data collected	2799	3293
Unique data	1950	1497
Observed data	1840	1175
GOF on F^2	1.078	1.00
Final R indices $[I > 2\sigma(I)]$	$R_1^a = 0.030$, $wR_2^b = 0.075$	$R_1^a = 0.041$, $wR_2^b = 0.098$
R indices (all data)	$R_1 = 0.032$, $wR_2 = 0.076$	$R_1 = 0.051$, $wR_2 = 0.102$

$R_1^a = \Sigma||F_o| - |F_c||/\Sigma|F_o|$. $wR_2^b = \{\Sigma[w(F_o^2 - F_c^2)^2]/\Sigma[w(F_o^2)^2]\}^{1/2}$, where $w = 1/[\sigma^2(F_o^2) + (0.0302P)^2 + 5.74P]$ with $P = (F_o^2 + F_c^2)/3$.

Table 2
Atomic coordinates ($\times 10^4$) and equivalent isotropic displacement parameters ($Å^2 \times 10^3$) for $La(HSeO_3)(SeO_4)$

	x	*y*	*z*	*U*(eq)
La(1)	2551(1)	3986(1)	2989(1)	6(1)
La(2)	−2392(1)	2140(1)	2963(1)	6(1)
Se(1)	637(1)	2198(2)	6065(1)	6(1)
Se(2)	5648(1)	3924(2)	6130(1)	6(1)
Se(3)	5102(1)	5597(2)	640(1)	9(1)
Se(4)	−409(1)	2972(2)	−243(1)	9(1)
O(1)	3732(7)	4515(10)	5902(6)	8(1)
O(2)	3172(8)	582(13)	3092(6)	11(1)
O(3)	1860(8)	548(13)	6797(7)	11(1)
O(4)	917(8)	4032(13)	7063(7)	12(1)
O(5)	736(7)	2599(11)	4399(6)	12(1)
O(6)	3968(8)	7023(13)	2937(7)	13(1)
O(7)	−1269(7)	1513(10)	5776(6)	8(1)
O(8)	5689(7)	3531(11)	4437(6)	10(1)
O(9)	3555(7)	5300(11)	−810(6)	12(1)
O(10)	6669(8)	4551(11)	17(7)	16(2)
O(11)	−310(7)	2544(10)	1524(6)	9(1)
O(12)	1758(7)	2718(10)	97(7)	13(1)
O(13)	4865(8)	3782(13)	1654(7)	13(1)
O(14)	951(7)	5982(10)	1061(6)	13(1)
H(1)	7503(3)	4572(2)	−140(4)	50
H(2)	4452(3)	6877(8)	2100(2)	50

Table 3
Atomic coordinates ($\times 10^4$) and equivalent isotropic displacement parameters ($Å^2 \times 10^3$) for $KNd(SeO_4)_2$

	x	*y*	*z*	*U*(eq)
Nd(1)	576(1)	1659(1)	3480(1)	9(1)
Se(1)	2821(1)	1579(1)	5893(1)	9(1)
Se(2)	−1910(1)	1635(1)	1076(1)	9(1)
K(1)	5662(2)	3564(3)	3406(2)	18(1)
O(1)	−1008(6)	7(7)	1872(5)	13(1)
O(2)	4118(7)	175(8)	6349(6)	23(1)
O(3)	1387(6)	−1581(7)	3070(5)	13(1)
O(4)	3048(6)	2558(7)	4571(5)	14(1)
O(5)	−1216(7)	3323(7)	4721(5)	17(1)
O(6)	−3738(6)	1474(7)	1024(6)	18(1)
O(7)	1190(6)	506(7)	5573(5)	14(1)
O(8)	2484(6)	3157(7)	6911(5)	17(1)

Tables 2 and 3. Further details of the crystal structure investigations can be obtained from the Fachinformationszentrum Karlsruhe, 76344 Eggenstein-Leopoldshafen, Germany, (fax: (49) 7247-808-666; e-mail: crysdata@fiz.karlsruhe.de) on quoting the depository number CSD 391294 and 391293.

3. Results and discussion

3.1. Synthesis

Reactions of selenic acid with the rare-earth salts in the presence of TEOS via the sol–gel method under the hydrothermal conditions, led to two new complexes with layered and framework structures, respectively. According to the experimental investigations, we noted that the sol–gel processing is the key factor for the preparation of such compounds. When the reactants cannot form the wet gels, the product only consists of the powder of the known compounds, $La_2(SeO_4)_3 \cdot 5H_2O$ or $Nd_2(SeO_4)_3 \cdot 5H_2O$, although all other conditions are kept constant. Additionally, it is of great interest that TEOS acts as a very subtle and important actor in the reaction process, as it is found that Si participates in the sol–gel process but is afterwards isolated from the products. All these indicate that the wet gels from TEOS provide a special reactive environment for selenic and rare-earth ions. As a result, these ions distributed evenly in the TEOS matrix and could self-assemble in the wet gels to form the crystals under suitable temperature conditions.

3.2. Crystal structure of $La(HSeO_3)(SeO_4)$

Selected bond distances and bond angles for compound **1** are listed in Table 4. $La(HSeO_3)(SeO_4)$ is the second well-characterized lanthanum compound containing both Se(IV) and Se(VI) oxyanions in the crystal structure. The asymmetric unit contains two independent lanthanum centers. La(1) is surrounded by ten oxygen atoms from five SeO_4^{2-} and three $HSeO_3^-$ groups with $d_{av}[La–O] = 2.62$ Å (Fig. 1a), defining the geometry of a distorted bicapped square antiprism. La(2) is in nine-fold coordination of oxygen atoms, each of which make a linkage to the selenium atoms ($d_{av}[La–O] = 2.59$ Å) (Fig. 1b). This coordination polyhedron can be best described as a monocapped square antiprism. Two independent selenium(IV) atoms with their lone pair of electrons are coordinated by three oxygen, forming a triangular pyramid $(SeO_3)^{2-}$ with Se^{4+} located at its apical corner ($d_{av}[Se(1)–O] = 1.71$ Å, $d_{av}[Se(2)–O] = 1.72$ Å), while two selenium (VI) atoms are tetrahedrally coordinated with bond lengths similar to those found in selenate compounds ($d_{av}[Se(3)–O] = 1.64$ Å, $d_{av}[Se(4)–O] = 1.64$ Å) (see Fig. 1).

The $La(1)O_{10}$ and $La(2)O_9$ polyhedra share two edges, O11–O8 and O13–O5, along the *a*-axis making up to a pseudo-1D lanthanum oxide chain of composition $[–La(1)O_{10}–La(2)O_9–La(1)O_{10}–La(2)O_9–]$ with a La–La minimum distance of 4.45 Å and similar crystallographic geometry like that observed in $La(HSeO_3)(SeO_4)(H_2O)_2$ [12]. However, while the single chains in the latter compound are isolated, the chains in compound **1** additionally share edges with the neighboring chains via La(1)–O(1)–La(2) and La(1)–O(7)–La(2) bridges, forming a puckered layer motif that stack perpendicular to the *c*-axis (Fig. 2). Numerous six-ring "windows" (i.e., a loop consisting of six edge-shared lanthanum polyhedra) are formed in this puckered layer,

Table 4
Selected bond distances (Å) and angles (°) in La($HSeO_3$)(SeO_4)

La(1)–O(14)	2.466(6)	La(2)–O(5)	2.706(6)
La(1)–O(5)	2.518(6)	Se(1)–O(4)	1.618(8)
La(1)–O(2)	2.520(10)	Se(1)–O(3)	1.626(8)
La(1)–O(6)	2.521(9)	Se(1)–O(5)	1.644(6)
La(1)–O(7)^{a}	2.575(7)	Se(1)–O(7)	1.664(6)
La(1)–O(13)	2.630(7)	Se(2)–O(2)^{e}	1.623(8)
La(1)–O(11)	2.707(6)	Se(2)–O(6)^{f}	1.628(9)
La(1)–O(8)	2.715(6)	Se(2)–O(8)	1.654(6)
La(1)–O(1)	2.736(6)	Se(2)–O(1)	1.660(6)
La(1)–O(12)	2.828(6)	Se(3)–O(9)	1.670(6)
La(2) O(9)^{b}	2.441(7)	Se(3)–O(13)	1.677(8)
La(2)–O(3)^{a}	2.511(9)	Se(3)–O(10)	1.776(7)
La(2)–O(11)	2.539(6)	Se(4)–O(14)^{b}	1.650(7)
La(2)–O(4)^{c}	2.587(9)	Se(4)–O(11)	1.700(6)
La(2)–O(1)^{c}	2.602(7)	Se(4)–O(12)	1.815(6)
La(2)–O(8)^{d}	2.631(6)	O(10)–H(1)	0.78(2)
La(2)–O(13)^{d}	2.649(7)	O(6)–H(2)	0.99(1)
La(2)–O(7)	2.655(6)		
O(14)–La(1)–O(5)	109.4(2)	O(1)^{c}–La(2)–O(5)	111.5(2)
O(14)–La(1)–O(2)	132.4(2)	O(7)–La(2)–O(5)	56.75(18)
O(5)–La(1)–O(2)	75.1(2)	O(11)–La(2)–O(7)	116.53(18)
O(2)–La(1)–O(6)	139.2(2)	O(9)^{b}–La(2)–O(5)	129.3(2)
O(5)–La(1)–O(7)^{a}	69.0(2)	O(4)–Se(1)–O(5)	113.0(4)
O(14)–La(1)–O(13)	90.9(2)	O(3)–Se(1)–O(5)	111.0(3)
O(2)–La(1)–O(13)	77.6(3)	O(3)–Se(1)–O(7)	110.6(4)
O(7)^{a}–La(1)–O(13)	136.8(3)	O(5)–Se(1)–O(7)	100.7(3)
O(6)–La(1)–O(11)	134.9(2)	O(2)^{e}–Se(2)–O(6)^{f}	111.1(4)
O(1)–La(1)–O(12)	167.2(2)	O(6)^{f}–Se(2)–O(8)	109.8(4)
O(9)^{b}–La(2)–O(3)^{a}	129.8(2)	O(8)–Se(2)–O(1)	100.7(3)
O(3)^{a}–La(2)–O(4)^{c}	141.1(2)	O(6)^{f}–Se(2)–O(1)	110.1(3)
O(9)^{b}–La(2)–O(1)^{c}	79.9(2)	O(9)–Se(3)–O(13)	101.0(3)
O(11)–La(2)–O(8)^{d}	150.8(2)	O(9)–Se(3)–O(10)	100.1(3)
O(3)^{a}–La(2)–O(13)^{d}	73.8(2)	O(13)–Se(3)–O(10)	94.3(4)
O(9)^{b}–La(2)–O(7)	136.5(2)	O(14)^{b}–Se(4)–O(11)	104.4(3)
O(4)^{b}–La(2)–O(7)	79.0(2)	O(14)^{a}–Se(4)–O(12)	98.5(3)
O(3)^{a}–La(2)–O(5)	72.5(2)	O(11)–Se(4)–O(12)	91.0(3)

[a] $-x,y+\frac{1}{2},-z+1$.
[b] $-x,y-\frac{1}{2},-z$.
[c] $-x,y-\frac{1}{2},-z+1$.
[d] $x-1,y,z$.
[e] $-x+1,y+\frac{1}{2},-z+1$.
[f] $-x+1,y-\frac{1}{2},-z+1$.

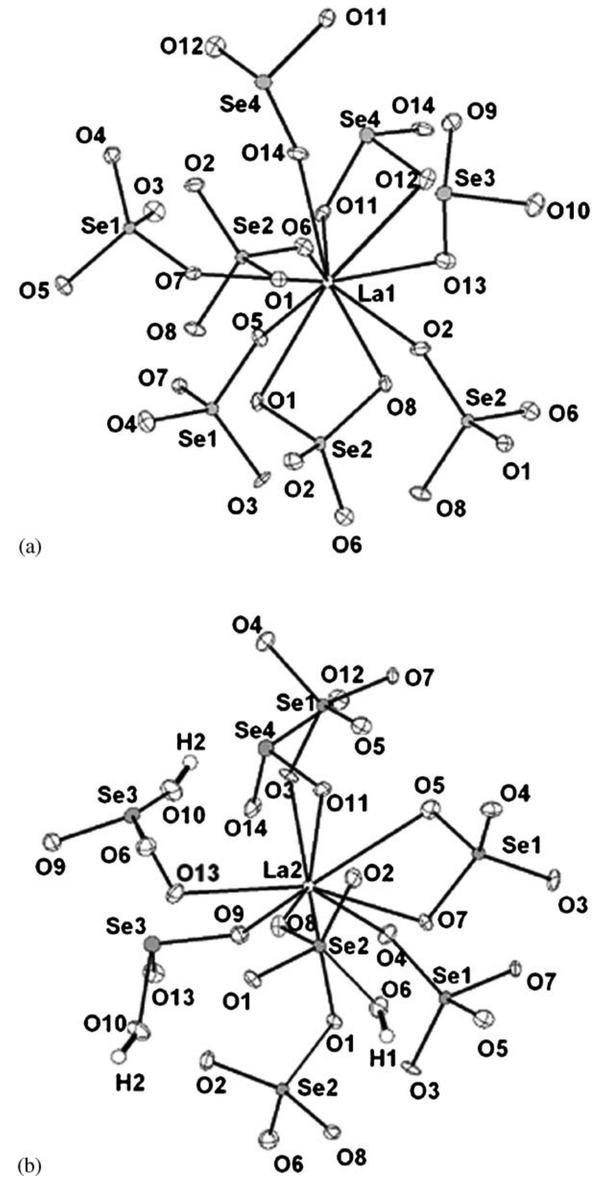

Fig. 1. Environments of La^{3+} ions in the crystal structure of La($HSeO_3$)(SeO_4): (a) coordination of La(1)O_{10}; and (b) coordination of La(2)O_9.

with the SeO_4 tetrahedra connected to each ring. Both edge and corner sharing are observed between the LaO_x ($x = 9, 10$) polyhedra and SeO_4 groups via one three-coordinated oxygen, O5, and two-coordinated oxygen, O3, O4 and O7, forming cationic $(LaSeO_4)^+$ sheets. Two distinct Se(IV) atoms of triangular pyramids $(SeO_3)^{2-}$ occupy the interspaces alternately and bridge the layers into a three-dimensional structure by Se–O–La bonds (Fig. 3). Two out of the three O atoms of Se(3)O_3 group make one bond with lanthanum cations from two adjacent sheets, respectively, while the remaining one is a protonated oxygen. On the other hand, each Se(4)O_3 group is edge-connected and corner-connected with two neighbouring layers. The triangular oxygen bases of these groups lie parallel to (0 1 0) and all $(SeO_3)^{2-}$ units are pointing in the same direction. Two hydrogen atoms sit on the oxygen O6 and O10, respectively, interact with the inorganic layers via hydrogen bonds (O6–H1…O13 = 2.43(2) Å, O10–H2…O11 = 2.59(2) Å).

3.3. Crystal structure of KNd(SeO_4)$_2$

Selected bond distances and bond angles of **2** are listed in Table 5. KNd(SeO_4)$_2$ is isostructural with KPr(SeO_4)$_2$ [6]. The structure can be considered as a layered structure with $[Nd(SeO_4)_2]^-$ groups, separated by K^+ cations. The Nd-atom coordinated by nine oxygen atoms within 3 Å (d_{av}[Nd–O] = 2.52(3) Å) (see

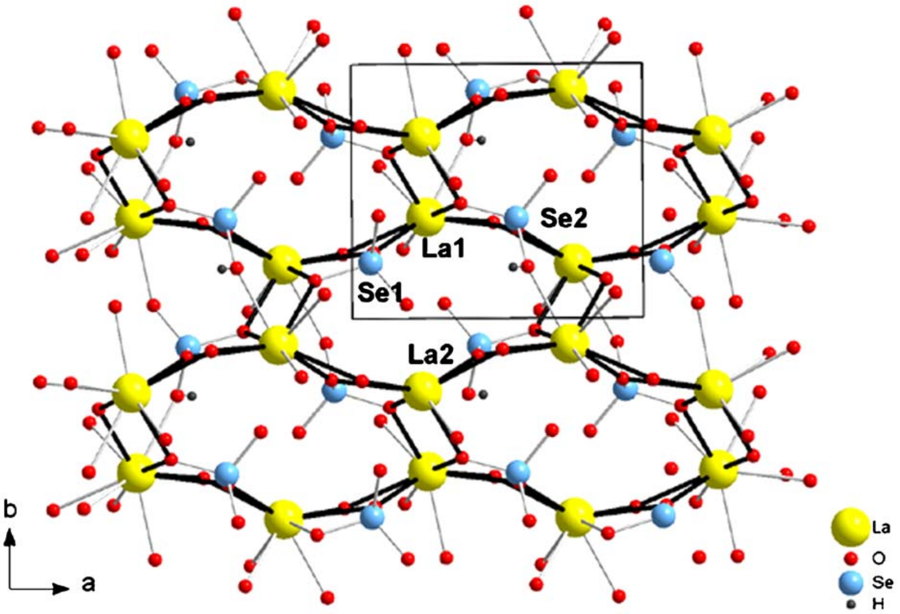

Fig. 2. Projection of La and Se network of La($HSeO_3$)(SeO_4) down the *c*-axis, showing the lanthanum polyhedral puckered layers with six-ring windows built from the edge-sharing LaO_x ($x = 9, 10$) units, and SeO_4 groups are located in the creases of the puckered layers, connecting with lanthanum cations by sharing edges and corners.

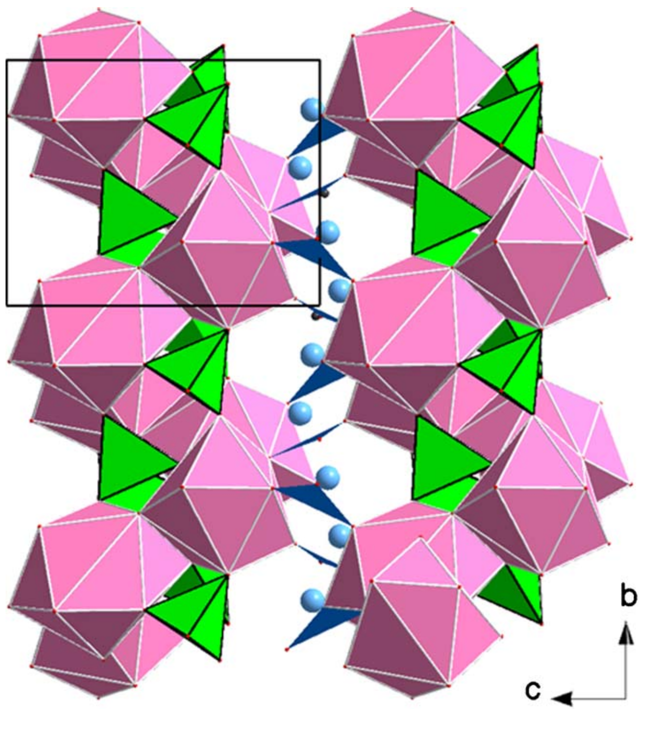

Fig. 3. Projection of La and Se network of La($HSeO_3$)(SeO_4) along the *a*-axis, showing that the puckered layers are edge- and corner-connected by the SeO_3 groups, which located in the interspaces of these layers (LaO_9 and LaO_{10} polyhedron, pink; SeO_4 tetrahedron, green; SeO_3, blue, Se atom, blue sphere, H atom, black sphere).

Fig. 4), exhibits the geometry of a monocapped square antiprism. Each NdO_9 polyhedron shares three edges with three neighboring neodymium groups to form NdO_9 polyhedral sheets with six-ring windows. SeO_4 tetrahedra are distributed on both sides of these sheets and connect with NdO_9 units through sharing one edge and one corner, leading to a "T–P–T" (tetrahedron–polyhedron–tetrahedron) layer (Fig. 5). The terminal oxygen atoms of SeO_4 tetraheda point toward the surface of each layer, giving rise to the lower

Table 5
Selected bond distances (Å) and angles (°) in KNd(SeO_4)$_2$

Nd(1)–O(6)	2.431(6)	Se(1)–O(2)	1.601(6)
Nd(1)–O(9)^a	2.435(6)	Se(1)–O(4)	1.642(5)
Nd(1)–O(3)	2.519(5)	Se(1)–O(8)	1.656(5)
Nd(1)–O(1)	2.531(5)	Se(1)–O(9)	1.644(6)
Nd(1)–O(1)^c	2.512(5)	Se(2)–O(7)	1.598(5)
Nd(1)–O(4)	2.531(5)	Se(2)–O(6)^a	1.627(6)
Nd(1)–O(3)^c	2.717(6)	Se(2)–O(1)	1.667(5)
Nd(1)–O(8)	2.506(5)	Se(2)–O(3)^c	1.668(5)
Nd(1)–O(8)^b	2.461(5)		
O(6)–Nd(1)–O(9)^a	146.43(18)	O(2)–Se(1)–O(4)	117.5(3)
O(9)^a–Nd(1)–O(8)^b	141.58(18)	O(2)–Se(1)–O(9)	111.8(3)
O(8)^b–Nd(1)–O(8)	60.8(2)	O(4)–Se(1)–O(9)	109.2(3)
O(8)–Nd(1)–O(3)	78.12(18)	O(9)–Se(1)–O(8)	108.2(3)
O(8)^b–Nd(1)–O(4)	119.97(17)	O(4)–Se(1)–O(8)	98.0(3)
O(3)–Nd(1)–O(4)	95.24(17)	O(7)–Se(2)–O(1)	115.0(3)
O(8)^b–Nd(1)–O(1)	69.75(17)	O(7)–Se(2)–O(6)^a	111.1(3)
O(3)–Nd(1)–O(1)	64.83(17)	O(6)^a–Se(2)–O(1)	108.5(3)
O(6)–Nd(1)–O(3)^c	73.38(17)	O(1)–Se(2)–O(3)^c	98.2(3)
O(4)–Nd(1)–O(3)^c	133.86(16)	O(6)^a–Se(2)–O(3)^c	113.7(3)

[a] $x, -y-\frac{1}{2}, z-\frac{1}{2}$.
[b] $-x, -y, -z+1$.
[c] $-x, y+\frac{1}{2}, -z+\frac{1}{2}$.

dimensionality of the structure. The guest K^+ ions occupy the interlayer space of layers to keep the structural stability and satisfy the charge balance (Fig. 6).

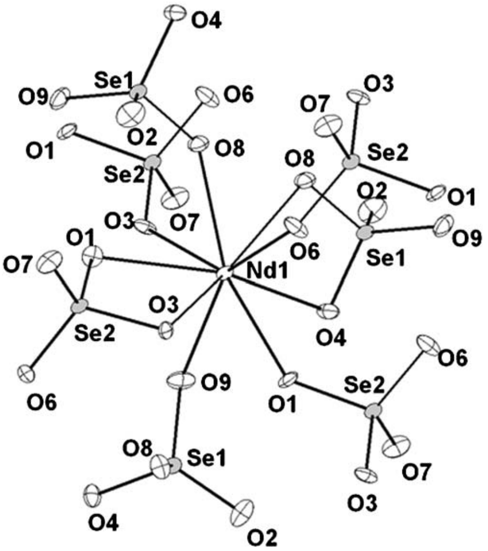

Fig. 4. Coordination of Nd^{3+} ions in the crystal structure of $KNd(SeO_4)_2$.

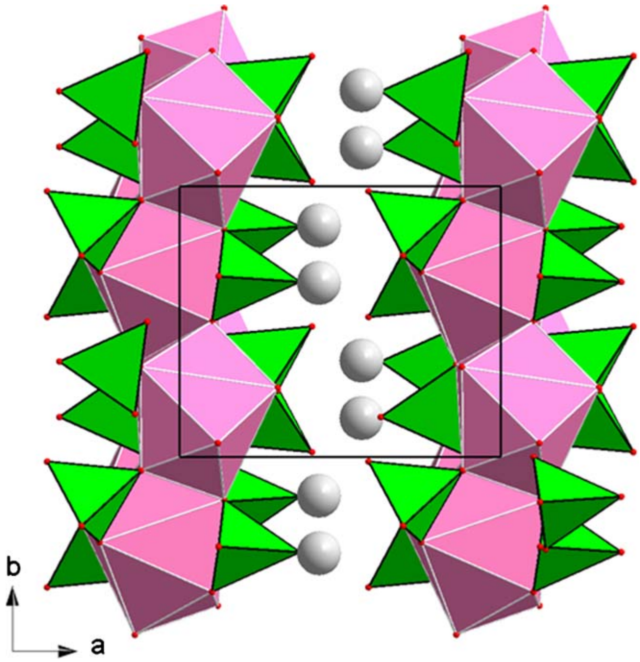

Fig. 6. Projection of Nd and Se network of $KNd(SeO_4)_2$ along the *c*-axis, showing the parallel stack of the inorganic layers in the [100] direction, and K^+ ions occupy the interspaces of layers (NdO_9 polyhedron, pink; SeO_4 tetrahedron, green; K atom, gray sphere).

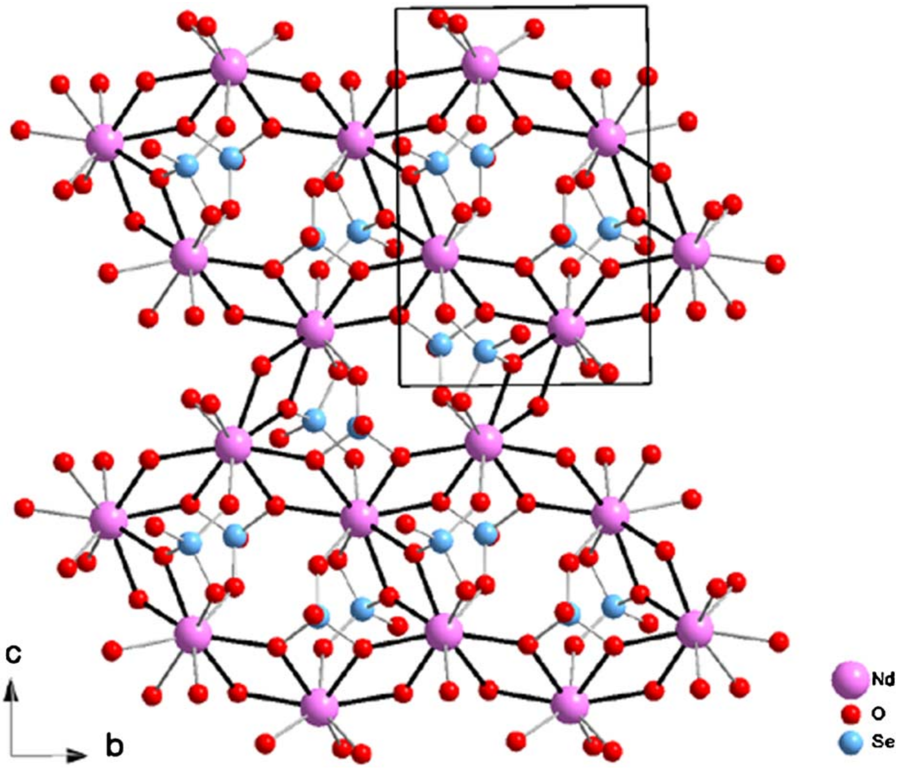

Fig. 5. Projection of Nd and Se network of $KNd(SeO_4)_2$ along the *a*-axis, showing the inorganic layers with six-ring windows built from the edge-sharing NdO_9 units, and SeO_4 groups occupy both sides of these layers linked via Se–O–Nd bonds.

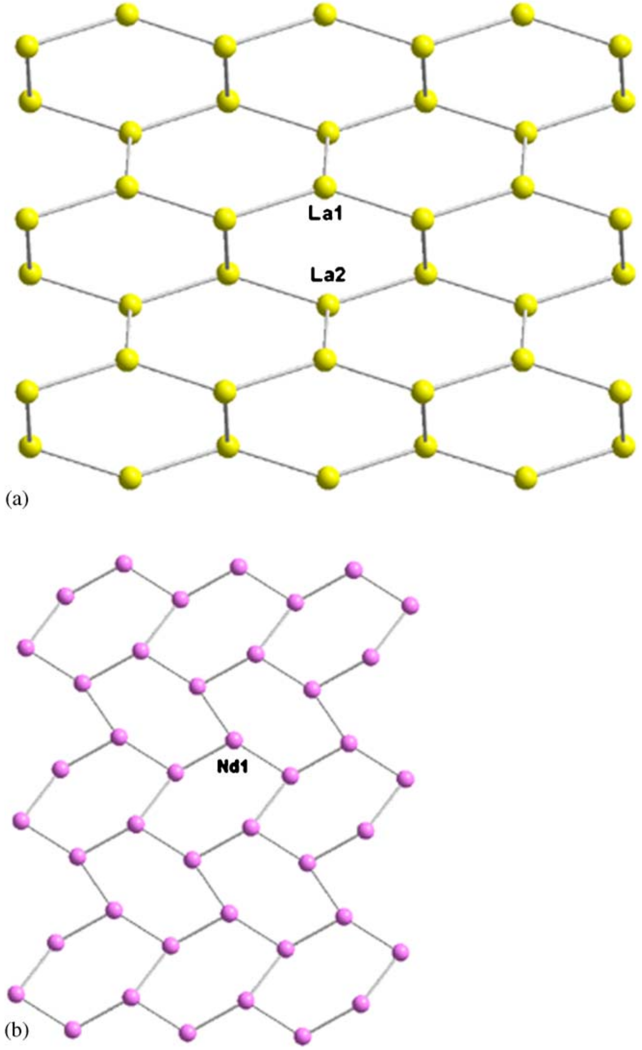

Fig. 7. Rare earth metal network with similar six-ring windows in the structures of $La(HSeO_3)(SeO_4)$ and $KNd(SeO_4)_2$: (a) the six-ring puckered network of La atoms in $La(HSeO_3)(SeO_4)$; and (b) the six-ring plane network of Nd atoms in $KNd(SeO_4)_2$.

A comparison of the two rare-earth compounds containing selenium atoms, examined in this manuscript, shows, that similar edge-shared rare-earth polyhedral networks with six-ring windows exist in both structures (Fig. 7). Additionally, these six-ring window networks in the title compounds exhibit different crystallographic features. Thus, $KNd(SeO_4)_2$ exhibits honey-comb like six rings, while the sheet of six-rings parallel to (0 1 1) in $La(HSeO_3)(SeO_4)$ is corrugated. Up to now, such puckered sheets have never been observed in rare earth selenites and selenates compounds. This strongly suggests that more materials with novel structures can be obtained by employing the sol–gel hydrothermal synthesis method presented here.

4. Conclusions

Two rare earth compound containing selenium atoms, $La(HSeO_3)(SeO_4)$ with a new open framework structure, and $KNd(SeO_4)_2$ with a layered structure have been synthesized under "Sol–gel" hydrothermal conditions for the first time. Similar edge-shared rare earth polyhedral networks with six-ring windows exist in both structures, yet have different stacking character (the former has puckered layers, while the latter has honeycomb like slabs), which indicates that the Si matrix might play an important role during the formation of these inorganic compounds. The successful syntheses of the two compounds not only further complete the family of rare earth selenite and selenate systems, but also provide important information for further developing novel rare earth selenites or selenates and related inorganic materials by using the sol–gel hydrothermal method.

Acknowledgments

This work was supported by the Fund for Distinguished Young Scholars (Inorganic Chemistry, No.20025101) and Key Project from the NNSF of China (No.50332050), State "863" project (No. 2002AA324070) and fund of Shanghai Optical Science and Technology (No. 022261015).

References

[1] J.J. Berzelius, Acad. Handl. Stockholm. 39 (1818) 13.
[2] J. Holsa, M. Leskela, J. Less Common Mer. 112 (1988) 127.
[3] S. Karvinen, L. Niinisto, Lanthanide Actinide Res. 1 (1986) 169.
[4] Y.M. Gasanov, L.D. Iskhakova, V.K. Trunov, Russ. J. Inorg. Chem. 30 (1985) 1731.
[5] S.M. Obanesyan, L.D. Iskhakova, V.K. Trunov, Russ. J. Inorg. Chem. 32 (1987) 896.
[6] L.D. Iskhakova, S.M. Ovanisyan, V.K. Trunov, Kristallografiya 35 (1990) 1083.
[7] R. Morris, W.T.A. Harrison, G.D. Stucky, A.K. Cheetham, Acta Crystallogr. C 48 (1992) 1182.
[8] A. Castro, R. Enjalbert, M. de Pedro, J.C. Trombe, J. Solid State Chem. 112 (1994) 418.
[9] I. Goehausen, M.S. Wickleder, Z. Anorg. Allg. Chem. 627 (2001) 1115.
[10] M.S. Wickleder, Z. Anorg, Allg. Chem. 626 (2000) 547.
[11] R.E. Morris, J.A. Hriljac, A.K. Cheetham, Acta Crystallogr. C 46 (1990) 2013.
[12] W.T.A. Harrison, Z. Zhang, Eur. J. Solid State Inorg. Chem. 34 (1997) 599.
[13] I. Kruegermann, M.S. Wickleder, Z. Anorg, Allg. Chem. 628 (2002) 147.
[14] R.E. Morris, A.P. Wilkinson, A.K. Cheetham, Inorg. Chem. 31 (1992) 4774.
[15] A.K. Cheetham, G. Ferey, T. Loiseau, Angew. Chem. Int. Ed. 38 (1999) 3268.
[16] A. Stein, W.S. Keller, T.E.K. Mallou, Science 259 (1993) 1558.
[17] T. Gopalakrishnan, Chem. Mater. 7 (1995) 1265.

[18] A. Yeganah-haeri, D.J. Weidner, I.B. Parise, Science 257 (1992) 650.

[19] (a) R.H. Blessing, Acta Crystallogr. A 51 (1995) 33;
(b) R.H. Blessing, SADABS: Area-Detector Absorption Correction, Bruker-AXS, Madison, WI, 1996.

[20] G.M. Sheldrick, SHELXS-97/2, Program for solution of crystal structures, University of Göttingen, Germany, 1997;
G.M. Sheldrick, SHELXL-97/2, Program for refinement of crystal structures, University of Göttingen, Germany, 1997.